Cellular/Molecular

The Residence Time of $GABA_A$Rs at Inhibitory Synapses Is Determined by Direct Binding of the Receptor α1 Subunit to Gephyrin

Jayanta Mukherjee,[1] Karla Kretschmannova,[1]* Geraldine Gouzer,[2]* Hans-Michael Maric,[3]* Sarah Ramsden,[4] Verena Tretter,[5] Kirsten Harvey,[4] Paul A. Davies,[1] Antoine Triller,[2] Hermann Schindelin,[3] and Stephen J. Moss[1,6]

[1]Department of Neuroscience, Tufts University School of Medicine, Boston, Massachusetts 02111, [2]Ecole Normale Supérieure, Inserm U1024, 75230 Paris Cedex 05, France, [3]Rudolf Virchow Center for Experimental Biomedicine, Institute of Structural Biology, University of Würzburg, 97080 Würzburg, Germany, [4]Department of Pharmacology, The School of Pharmacy, London WC1N 1AX, United Kingdom, [5]Department of Biochemistry and Molecular Biology, Medical University Vienna Center for Brain Research, 1090 Vienna, Austria, and [6]Department of Neuroscience, Physiology and Pharmacology, University College, London WC1 6BT, United Kingdom

The majority of fast synaptic inhibition in the brain is mediated by benzodiazepine-sensitive α1-subunit-containing GABA type A receptors ($GABA_A$Rs); however, our knowledge of the mechanisms neurons use to regulate their synaptic accumulation is rudimentary. Using immunoprecipitation, we demonstrate that $GABA_A$Rs and gephyrin are intimately associated at inhibitory synapses in cultured rat neurons. *In vitro* we reveal that the E-domain of gephyrin directly binds to the α1 subunit with an affinity of ~20 μM, mediated by residues 360–375 within the intracellular domain of this receptor subunit. Mutating residues 360–375 decreases both the accumulation of α1-containing $GABA_A$Rs at gephyrin-positive inhibitory synapses in hippocampal neurons and the amplitude of mIPSCs. We also demonstrate that the affinity of gephyrin for the α1 subunit is modulated by Thr375, a putative phosphorylation site. Mutation of Thr375 to a phosphomimetic, negatively charged amino acid decreases both the affinity of the α1 subunit for gephyrin, and therefore receptor accumulation at synapses, and the amplitude of mIPSCs. Finally, single-particle tracking reveals that gephyrin reduces the diffusion of α1-subunit-containing $GABA_A$Rs specifically at inhibitory synapses, thereby increasing their confinement at these structures. Our results suggest that the direct binding of gephyrin to residues 360–375 of the α1 subunit and its modulation are likely to be important determinants for the stabilization of $GABA_A$Rs at synaptic sites, thereby modulating the strength of synaptic inhibition.

Introduction

GABA type A receptors ($GABA_A$Rs) mediate fast neuronal inhibition in the brain and are the sites of action for benzodiazepines (Sieghart and Sperk, 2002; Rudolph and Mohler, 2006). $GABA_A$Rs are heteropentameric, chloride-selective, ligand-gated ion channels that can be assembled from a large repertoire of subunit classes with multiple members: α1–α6, β1–β3, γ1–γ3, δ, ε, θ, π, and ρ1–ρ3. This provides the basis for extensive structural heterogeneity (Luscher and Keller, 2004; Jacob et al., 2008). While the significance of $GABA_A$R structural diversity is not fully understood, it is broadly accepted that the majority of benzodiazepine-sensitive synaptic $GABA_A$R subtypes are composed of α1–α6, β1–β3, and γ2 subunits with an excess of 55% of this population being composed of α1, β2, γ2 subunits (Benke et al., 1994; McKernan and Whiting, 1996; Jacob et al., 2008). Receptors composed of α4–α6/β, with or without δ subunits, are believed to form a specialized population of extrasynaptic receptors that mediate tonic inhibition (Farrant and Nusser, 2005; Glykys and Mody, 2007; Jacob et al., 2008).

Central to the efficacy of phasic inhibition is the selective accumulation of the appropriate $GABA_A$R subtypes at postsynaptic inhibitory sites. One protein that is consistently implicated in these processes is gephyrin. Gephyrin was first characterized as a binding partner for glycine receptors (GlyRs), linking them to the cytoskeleton via an interaction with a specific hydrophobic amino acid motif within the intracellular domain of the GlyR β subunit (Pfeiffer et al., 1982; Kneussel and Betz, 2000; Kim et al., 2006). Gephyrin is enriched at postsynaptic inhibitory specializations throughout the brain and colocalizes with $GABA_A$R subtypes that incorporate α1–α3, β2, β3, and γ2 subunits (Sassoe-Pognetto et al.,1995; Sassoe-Pognetto and Fritschy, 2000).

The role that gephyrin plays in regulating the synaptic clustering of $GABA_A$Rs has been addressed using gephyrin knock-out mice, antisense oligonucleotide, RNA_i, and gephyrin deletion. Initial reports suggested a critical role for gephyrin in regulating the clustering of most $GABA_A$R subtypes (Essrich et al., 1998;

Received April 12, 2011; revised Aug. 16, 2011; accepted Aug. 20, 2011.

Author contributions: J.M., K.K., K.H., A.T., H.S., and S.J.M. designed research; J.M., K.K., G.G., H.-M.M., and S.R. performed research; J.M., K.K., G.G., H.-M.M., V.T., K.H., P.A.D., A.T., H.S., and S.J.M. analyzed data; J.M., K.K., G.G., A.T., H.S., and S.J.M. wrote the paper.

This work was supported by National Institute of Neurological Disorders and Stroke Grants NS047478, NS48045, NS051195, NS054900, NS056359, and NS065725 and a Sponsored Research Agreement from AstraZeneca. The work of H.S. was supported by Deutsche Forschungsgemeinschaft Grants FZ 82 and SFB 487C7. A.T. was supported by Fondation de la Recherche Médicale and Agence National de la Recherche Grant ANR-R08072JJ.

*K.K., G.G., and H.-M.M. contributed equally to this work.

Correspondence should be addressed to Stephen J. Moss at the above address. E-mail: stephen.moss@tufts.edu.

DOI:10.1523/JNEUROSCI.2001-11.2011

 0270-6474/11/3114677-11$15.00/0

Kneussel et al., 1999; Fischer et al., 2000; Jacob et al., 2005). In contrast, more recent observations suggest that gephyrin is not required for the synaptic clustering of the most abundant benzodiazepine-sensitive $GABA_AR$ subtypes in the brain, namely, those that contain α1 subunits (Kneussel et al., 2001; Levi et al., 2004; Yu et al., 2007). Thus, it remains to be determined how the most abundant subtype of benzodiazepine-sensitive $GABA_AR$ subtypes are stabilized enriched at inhibitory synapses.

We demonstrate here that gephyrin binds directly to the intracellular domain of the α1 subunit with an affinity of ~20 μM, an interaction that is critically dependent on intracellular residues 360–375 of the α1 subunit including Thr375, a putative phosphorylation site. In cultured neurons, gephyrin facilitates the synaptic accumulation of $GABA_ARs$ by selectively reducing their diffusion, thus increasing their dwell time at inhibitory synapses. Collectively, our results provide evidence that the direct binding of the α1 subunit to gephyrin is likely to play a central role in regulating the accumulation of the majority of benzodiazepine-sensitive $GABA_ARs$ at inhibitory synapses.

Materials and Methods

cDNA constructs, fusion proteins, and antibodies. A full-length mouse α1 $GABA_AR$ subunit, modified with an N-terminal pHluorin, has been described previously (Connolly et al., 1999; Bogdanov et al., 2006; Tretter et al., 2008). Mutations, deletions, and glutathione *S*-transferase (GST) fusion protein expression were performed as detailed previously (Tretter et al., 2008). Monoclonal gephyrin antibodies were purchased from Synaptic Systems. Rabbit polyclonal vesicular inhibitory amino acid transporter (VIAAT) antibody was a generous gift from Dr. Bruno Gasnier (Centre National de la Recherché Scientifique, Paris, France). GFP antibody (mouse monoclonal) was purchased from Roche Diagnostics. A monoclonal antibody raised against the M3-M5 loop of the $GABA_AR$ α1 subunit was purchased from Antibodies Inc.

Cell culture, detergent solubilization, coimmunoprecipitation, and Western blotting. Hippocampal cultured neurons were prepared and nucleofected as described previously from embryonic day 18 rat embryos of either sex (Kittler et al., 2004; Jacob et al., 2005). For immunoprecipitation, cultures were solubilized in 5 mM EGTA; 5 mM EDTA; 50 mM NaCl; 50 mM Na_3PO_4, pH 7.5; 2 mM PMSF; 5 mM benzamidine; 10 μg/ml each of aprotinin, leupeptin, and pepstatin; and 2% Triton X-100 at 4°C for 2 h. Extracts were then immunoprecipitated using the M3–M4 loop-specific α1 antibody coupled to protein G-Sepharose (GE Healthcare) (Connolly et al., 1996). Immunoblots were visualized using ECL followed by analysis using the CCD-based FujiFilm LAS 3000 system (Abramian et al., 2010).

Protein overlay assay. Fusion proteins (2–5 μg) were subjected to SDS-PAGE and transferred to a nitrocellulose membrane. The membrane was renatured using a gradient of guanidine hydrochloride (7.5–0 M) and then incubated in overlay buffer (10 mM HEPES, pH 7.5, 70 mM KCl, 5 mM EDTA, 2% BSA) for 1 h. It was then incubated with ^{35}S-methionine gephyrin (10^6 cpm/ml; P1 isoform) labeled using the TNT T7 Quick-Coupled Transcription/Translation kit (Promega) overnight at 4°C. Membranes were washed extensively in overlay buffer, and binding was quantified using a phosphoimager combined with Coomassie staining (Tretter et al., 2008).

Isothermal titration calorimetry. For isothermal titration calorimetry (ITC) experiments, the cytoplasmic loop located between transmembrane (TM) helices 3 and 4 of the α1 subunit and its variants were PCR amplified from pRK5 plasmids and the fragments inserted into the *Nco*I/*Not*I sites of the pETM-11 vector. $GABA_AR$ α1-loop variants were expressed in *Escherichia coli* BL21 cells (Stratagene) as "6-His"-tagged proteins. Cells were grown in LB medium at 30°C, and protein expression was induced with 0.5 mM isopropyl β-D-1-thiogalactopyranoside for 18 h. Cells were resuspended in the appropriate lysis buffer, passed through a cell disruptor (Constant Systems), and centrifuged. Proteins were initially purified using a 5 ml HisTrap FF crude column according to the manufacturer's instructions (GE Healthcare). Protein-containing fractions were collected, concentrated, and applied to a 26/60 Superdex 200 size exclusion chromatography column (GE Healthcare) equilibrated with buffer (10 mM Tris/HCl, 250 mM NaCl, pH 8.0). Pure fractions were pooled, concentrated to 5–100 mg/ml, flash frozen in liquid nitrogen in 0.5 ml aliquots, and stored at −80°C. The E-domain of gephyrin (Geph-E) was purified as described previously (Schrader et al., 2004; Kim et al., 2006).

Before all ITC experiments, the gephyrin and $GABA_AR$ α1-loop samples were extensively dialyzed against identical buffer (10 mM Tris–HCl, 250 mM NaCl, 1 mM β-mercaptoethanol, pH 8.0) at 4°C overnight, followed by ultrafiltration and degassing. Three hundred microliters of $GABA_AR$ α1 loops (230–1640 μM) were titrated as the ligand into the sample cell containing 1.5 ml of Geph-E (12.5–100 μM, respectively). A volume 10–15 μl of ligand was added at a time, with a total number of 20–30 injections, resulting in a final molar ligand-to-protein ratio varying between 3:1 and 6:1. All experiments were performed using a VP-ITC instrument (MicroCal) at 25°C. Buffer-to-buffer titrations were performed as described above so that the heat produced by injection, mixing, and dilution could be subtracted before curve fitting. The binding enthalpy was measured directly, while the association constants (K_a) and stoichiometries (N) were obtained by data analysis using Origin software, using a one-site binding model.

Yeast two-hybrid assays. The yeast strain Y190 was cotransformed with pYTH16-$GABA_AR$ with either wild-type or mutant α1 subunit intracellular M3–M4 loop constructs as bait together with pACT2-gephyrin prey constructs. pACT2-gephyrin deletion mutants have been described previously (Harvey et al., 2004; Saiepour et al., 2010). Transformations were plated on selective dropout media (either −LeuTrpHis plus 30 mM 3-AT or −LeuTrp). After incubation at 30°C for 3–6 d, *LacZ* reporter gene assays were performed as described previously (Harvey et al., 2004; Saiepour et al. 2010).

Confocal microscopy and image analysis. All imaging experiments were performed using 18–21 d *in vitro* (DIV) rat hippocampal cultures. For immunostaining, cultures were fixed, permeabilized with 0.4% Triton X-100, and incubated with the respective primary antibodies and subsequently with fluorescently labeled secondary antibodies (Jackson ImmunoResearch). Images were acquired using a Nikon Eclipse Ti series confocal microscope with a 60× objective (NA, 1.4) and analyzed using MetaMorph software (Molecular Devices) (Jacob et al., 2005). In our experiments, a receptor cluster was defined as being ~0.5 μm^2 and approximately twofold to threefold more intense than background diffuse fluorescence. Synaptic clusters were colocalized with or directly apposed to VIAAT staining. Analyses are based upon the number of cells (n) from at least three independent cultures.

Single-particle tracking and analysis. Rat hippocampal neurons were cotransfected with $^{pH}\alpha$1 or $^{pH}\alpha$1/6 and monomeric RFP (mRFP)-gephyrin (Hanus et al., 2006) at 9 DIV using lipofectamine 2000 (Invitrogen) and following the manufacturer's instructions. Single-particle tracking (SPT) was performed at 21–24 DIV. Cells were labeled and imaged at 37°C in MEM for recording (phenol red-free MEM, 33 mM glucose, 20 mM HEPES, 2 mM glutamine, 1 mM Na-pyruvate, and 1× B27). Quantum dots (QDs) emitting at 655 nm conjugated with goat $F(ab')_2$ anti-rabbit IgG (Invitrogen) were previously coupled to an anti-GFP antibody (rabbit polyclonal; Synaptic Systems) as described previously (Renner et al., 2009). Cells were incubated for 10 min at 37°C with the precoupled QDs (0.2 nM) and then rinsed. Cells were then imaged in an open chamber mounted on an Olympus IX70 inverted microscope equipped with a 60× objective (NA, 1.45). Fluorescence was detected using a mercury lamp, appropriate excitation and emission filters (QDs, FF01-460/60-25, FF01-655/15-25; mRFP, FF01-560/25-25, FF01-607/36-27, Semrock; pHluorin, HQ500/20 and HQ535/30m, Chroma Technology via Roper Scientific), a CCD camera (Cascade 512BFT; Roper Scientific), and MetaVue (Molecular Devices). Recordings were performed within 30 min after QD staining.

Analysis of SPT experiments was performed with custom software using Matlab (MathWorks). The center of the QD fluorescent spot was determined with a spatial accuracy of ~10 nm using a 2D-Gaussian fit. Trajectories were reconstructed as described previously (Hanus et al., 2006). QDs with trajectories ≥15 points were retained for quantitative analysis. Values of mean square displacement (MSD) versus time (t) were calculated using the following formula: $MSD(ndt) = (N-n)^{-1}\sum_{i=1}^{N-n}((x_{i+n}-x_i)^2 + (y_{i+n}-y_i)^2)$, where x_i and y_i are the coordinates of a dot on frame i, N is the

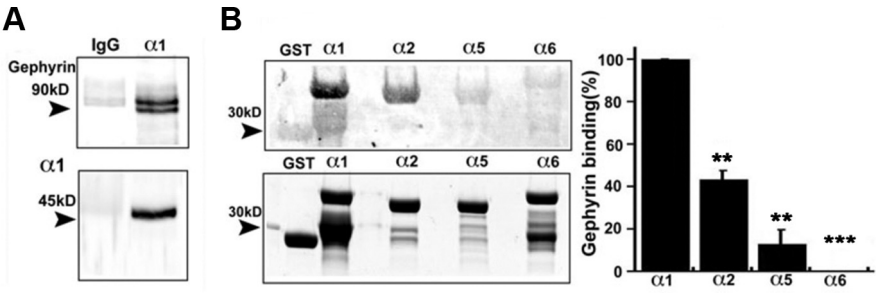

Figure 1. α1-subunit-containing GABA$_A$Rs are intimately associated with gephyrin. ***A***, Lysates from 18–21 Div neurons were immunoprecipitated with anti-α1 or IgG. Precipitated material was immunoblotted with gephyrin (top) or anti-α1 (bottom) antibodies. ***B***, A total of 2.5 μg of the respective fusion proteins was overlaid with ^{35}S-gephyrin. The top shows an autoradiograph, and the bottom shows Coomassie staining of the same gel. The level of gephyrin binding was corrected for input and normalized to the level seen for the α1 subunit (α1 = 100%). Data are presented as mean ± SEM. $^{**}p < 0.01$; $^{***}p < 0.001$ (unpaired *t* test; $n = 3$).

total number of steps in the trajectory, *dt* is the time between two successive frames, and *ndt* is the time interval over which displacement is averaged (Triller and Choquet, 2008). Diffusion coefficients (D) were calculated by fitting the first five points of the MSD versus time curve with the equation MSD = $4Dt$. For the square step analysis, the displacements for 1 s time intervals were calculated all along the trajectories using the formula $r_t^2 = (x_t - x_{t+1s})^2 + (y_t - y_{t+1s})^2$. Synaptic images were filtered using a multidimensional image analysis interface run by MetaMorph software. Spots were classified as synaptic when they colocalized with mRFP-gephyrin clusters.

Electrophysiology. For electrophysiological measurements, neurons were nucleofected with pHluorin-tagged constructs. Cells were plated on 12 mm glass coverslips (German glass; VWR) coated with poly-L-lysine (0.5 mg/ml; Sigma) and cultured for 2–3 weeks before the recordings. To measure mIPSCs, coverslips were placed in a recording chamber mounted on the stage of an inverted microscope and continuously perfused with extracellular solution containing the following (in mM): 150 NaCl, 4.7 KCl, 2.5 $CaCl_2$, 1.2 $MgCl_2$, 10 HEPES, and 11 glucose, adjusted to pH 7.4 with NaOH, with osmolality 295–315 mmol/kg. Excitatory and action potentials were blocked by the addition of 10 μM DNQX, 25 μM D-AP-5, and 0.3 μM TTX (Tocris Bioscience). The bath solution was heated to 32–33°C by an in-line heater (Warner Instruments). Patch pipettes were pulled from borosilicate glass (World Precision Instruments) and filled with intracellular solution containing the following (in mM): 150 CsCl, 2 $MgCl_2$, 0.1 $CaCl_2$, 10 HEPES, 1.1 EGTA, and 2 Mg-ATP, adjusted to pH 7.2 with CsOH, with osmolality 275–290 mmol/kg. After establishing whole-cell conditions, a period of 3 min was allowed to stabilize recordings before collecting data. Recordings were made at a holding potential of −70 mV. Synaptic currents were recorded using an Axopatch 200B amplifier (Molecular Devices), low-pass filtered at 2 kHz, digitized (10 kHz; Digidata 1320A; Molecular Devices), and stored for off-line analysis. Access resistance (<15 MΩ; 65–75% compensation) was monitored throughout the recordings, and data from the cell were discarded when a change of >20% occurred. Amplitude, frequency, decay (τ), and 10–90% rise time of mIPSCs were analyzed using Mini Analysis software (Synaptosoft). For decay and 10–90% rise time, 50 events without superposition were selected per cell and averaged. The decay was fitted with a biexponential curve, and the weighted decay (τ_w) was calculated using the equation $\tau_w = (\tau_1 * A1) + (\tau_2 * A2)/(A1 + A2)$, where A1 and A2 are amplitudes of fast and slow decay components, and τ_1 and τ_2 are their respective decay time constants. Unless indicated otherwise, data are expressed as mean ± SEM; *p* values represent the results of independent *t* tests.

Results

Gephyrin and α1-subunit-containing GABA$_A$Rs are intimately associated at inhibitory synapses

Immunolocalization has revealed that gephyrin and α1-subunit-containing GABA$_A$Rs colocalize at inhibitory synapses in many brain regions and in culture (Essrich et al., 1998; Kneussel et al., 1999; Sassoe-Pognetto and Fritschy, 2000; Brunig et al., 2002; Danglot et al., 2003). However, whether these proteins directly interact with each other in biochemical assays remained to be established. To test this extracts of 18–21 DIV cortical neurons were subjected to immunoprecipitation using a monoclonal antibody against an epitope within the intracellular domain of the α1 subunit (NeuroMab; anti-α1) or control IgG. Precipitated material was then immunoblotted with antibodies against gephyrin and anti-α1. A doublet centered on 93 kDa was seen with gephyrin antibodies in lysates exposed to anti-α1 but not control IgG. α1 subunit immunoreactivity was also evident in material immunoprecipitating with anti-α1 but not control IgG (Fig. 1*A*). Our results thus reveal that gephyrin and α1-subunit-containing GABA$_A$Rs are intimately associated in cultured neurons.

Gephyrin binds directly to the α1 subunit and requires residues 360–375

To determine whether the association of gephyrin and the α1 subunit is mediated via direct binding, we expressed the intracellular loop between TM regions 3 and 4 of a range of GABA$_A$Rs as GST fusion proteins. The respective fusion proteins were then overlaid with the P1 isoform of gephyrin, which was labeled with ^{35}S-methionine (Bedford et al., 2001; Tretter et al., 2008). Binding of gephyrin to GST-α1 could be demonstrated under these conditions (normalized to 100%). Binding of gephyrin to GST-α1 could be demonstrated under these conditions (normalized to 100%) but not to GST alone and significantly lower levels of binding were also seen to the α2 subunit (43.7 ± 3.8% of GST-α1, $p \leq 0.005$, *t* test, $n = 3$) (Fig. 1*B*). We further examined the specificity of gephyrin binding to GABA$_A$Rs by measuring interactions with the intracellular domains of the α5 and α6 subunits, which are believed to be components of receptor subtypes that mediate tonic inhibition at extrasynaptic sites and are excluded from gephyrin-positive synapses (Brickley et al., 2001; Farrant and Nusser, 2005; Glykys et al., 2008). In contrast to the α1 and α2 subunits, only minimal levels of gephyrin binding (12.9 ± 7% of control; $p \leq 0.005$, *t* test; $n = 3$) for α5 and no detectable binding for α6 subunits ($p < 0.001$, *t* test; $n = 3$) to the respective fusion proteins was seen (Fig. 1*B*, right).

To gain information on the binding site(s) for gephyrin within the α1 subunit, we constructed two smaller fusion proteins encoding the N- and C-terminal domains of the α1 intracellular loop. This revealed that the amino acids critical for gephyrin binding lie between residues 334 and 375 (Fig. 2*A*). To gain further insights into the gephyrin binding site, we deleted residues 360–375 (LIKKNNTYAPTATSYT) since the homologous region in the α2 subunit has been strongly implicated in gephyrin binding (Fig. 2*B*) (Tretter et al., 2008). Deletion of residues 360–375 (α1Δ1) significantly reduced gephyrin binding ($p \leq 0.002$, *t* test; $n = 3$). This effect is specific because deletion of residues 384 to 395 (α1Δ2) had no effect (Fig. 2*A*). To further control for the possible deleterious effects of the respective deletions on protein folding, we exchanged residues 360–375 in the α1 subunit for the corresponding region of the α6 subunit (α1/6) since the α6 subunit does not bind to gephyrin. Consistent with the results seen with GST-α1Δ1, significantly lower levels of gephyrin binding

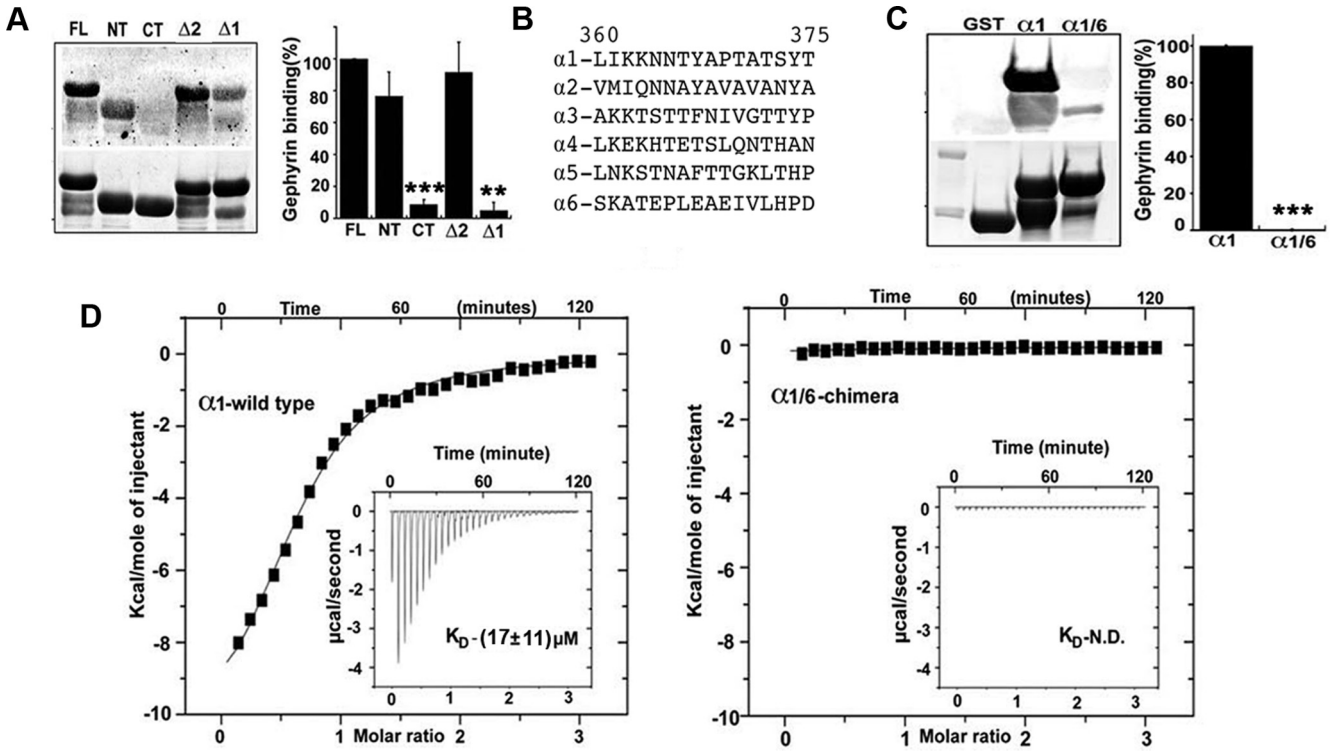

Figure 2. Residues 360–375 within the α1 subunit mediate high-affinity binding to gephyrin. ***A***, Fusion proteins encoding distinct portions of the intracellular domain of the α1 subunit were overlaid with ^{35}S-gephyrin. Left, The top shows an autoradiograph, and the bottom shows Coomassie staining of the same gel. The level of gephyrin binding was corrected for input and normalized to the level seen for the α1 subunit (α1 = 100%). FL, Full length M3–M4 loop; NT, N-terminal half (334–375); CT, C-terminal half (376–419); Δ1, deletion 1 (360–375); Δ2, deletion 2 (384–395); α1, GST fusion protein. ***B***, Alignment of homologous regions of α1 subunits of residues 360–375 of the α1 subunit. ***C***, Overlay assays were performed using GST-α1 and GST-α1/6, and data were normalized to the level of binding seen for α1 (100%). Data represent mean ± SEM. ***$p < 0.001$ (unpaired t test; $n = 3$). ***D***, Binding affinities were determined in ITC experiments by titrating the gephyrin E-domain (309–750, P1 variant) with α1 or α1/6 under similar experimental conditions. The measured binding enthalpies are plotted as a function of the molar ratio of the respective fusion proteins. Heat release over time is shown in the inset together with the average K_D and its SD. N.D., Not detectable.

were seen to GST-α1/6 compared to GST-α1 (Fig. 2*C*) ($p < 0.001$, t test; $n = 3$).

To determine the affinity of the α1 subunit for gephyrin, we used ITC. For this experiment, the intracellular domain of the α1 subunit was expressed in *E. coli* as a 6×HIS fusion protein. After purification, binding to the E-domain of gephyrin (residues 309–750) was analyzed. This domain of gephyrin was used because it binds to the β subunit of GlyRs with an affinity similar to that seen for the full-length protein. Specifically, two binding sites with affinities of 0.14 ± 0.08 and 7.7 ± 0.08 μM were seen for GlyRβ binding to gephyrin (Schrader et al., 2004; Kim et al., 2006). ITC revealed that the intracellular domain of the α1 subunit binds to the E-domain of gephyrin with a K_D of 17 ± 11 μM ($n = 11$) and a stoichiometry of 0.66 mol/mol (Fig. 2*D*); however, no binding was seen to α1/6 (Fig. 2*D*; Table 1). Collectively, these results suggest that residues 360–375 of the α1 subunit are essential in mediating binding to gephyrin. It is interesting to note that residues 360–375 are 31% identical and 43% similar among the α1, α2, and α3 subunits but are not conserved in the α4–α6 subunits (Fig. 2*B*), suggesting a conserved mechanism of gephyrin binding. It would of course be of interest to compare the affinities of the α1 and α2 subunits for gephyrin; however, this comparison could not be performed since we have not been successful in obtaining the necessary large amounts of the α2 fusion protein.

Table 1. Analysis of the binding of gephyrin to the intracellular domains of GlyR β and α1 subunit intracellular domains

Receptor loop (M3–M4)	Stoichiometry (N)	Affinity (in μM)	Enthalpy (in kcal/mol)	Measurements
GlyR β WT[a]	0.65 ± 0.01	0.14 ± 0.08	−16 ± 1	1
	0.60 ± 0.2	7.7 ± 0.1	−7 ± 2	
GABA$_A$R α1 WT[b]	0.62 ± 0.07	17 ± 11	−6 ± 7	11
GABA$_A$R α1/6 chimera[b]	N.D.	N.D.	N.D.	2
GABA$_A$R α1 T375E[b]	0.69 ± 0.001	183 ± 33	−6 ± 8	2
GABA$_A$R α1 T375A[b]	0.64 ± 0.028	36 ± 11	−15 ± 15	2

Purified fusion proteins encoding the intracellular domains of GlyR and GABA$_A$R subunits were exposed to the residues 309–750 of the P1 variant of gephyrin, and the interaction was measured using ITC. All values represent mean ± SD; $n = 11$ for wild type (WT) and $n = 2$ for mutants. N.D., Not detectable.

[a]Analyzed with a two-site binding model. Top numbers refer to the high-affinity binding site. Data were taken from the study by Kim et al. (2006) for a representative measurement with SDs derived from the curve-fitting procedure in Origin.

[b]Analyzed with a single-site binding model. Mean values were calculated for several α1 measurements and are given with their SDs.

Preventing gephyrin binding to the α1 subunit blocks the synaptic clustering of GABA$_A$Rs

To examine the significance of gephyrin binding, we compared the synaptic accumulation of full-length wild-type and mutant α1 subunits modified with N-terminal pHluorin reporters, modifications that do not compromise functional expression of the receptor ($^{pH}\alpha$1 and $^{pH}\alpha$1/6, respectively) (Bogdanov et al., 2006; Twelvetrees et al. 2010). Expressing neurons (18–21 DIV) were fixed, permeabilized, and stained with VIAAT and gephyrin antibodies. They were then examined using confocal microscopy. Punctae of $^{pH}\alpha$1 immunoreactivity were evident that precisely colocalized with gephyrin. These structures were enriched at inhibitory synapses as defined by their colocalization with VIAAT. In contrast, $^{pH}\alpha$1/6-containing receptors appeared to show a deficit in synaptic accumulation (Fig. 3*A*). A significant decrease (Fig. 3*A*) in the number of $^{pH}\alpha$1/6 clusters per unit length (30

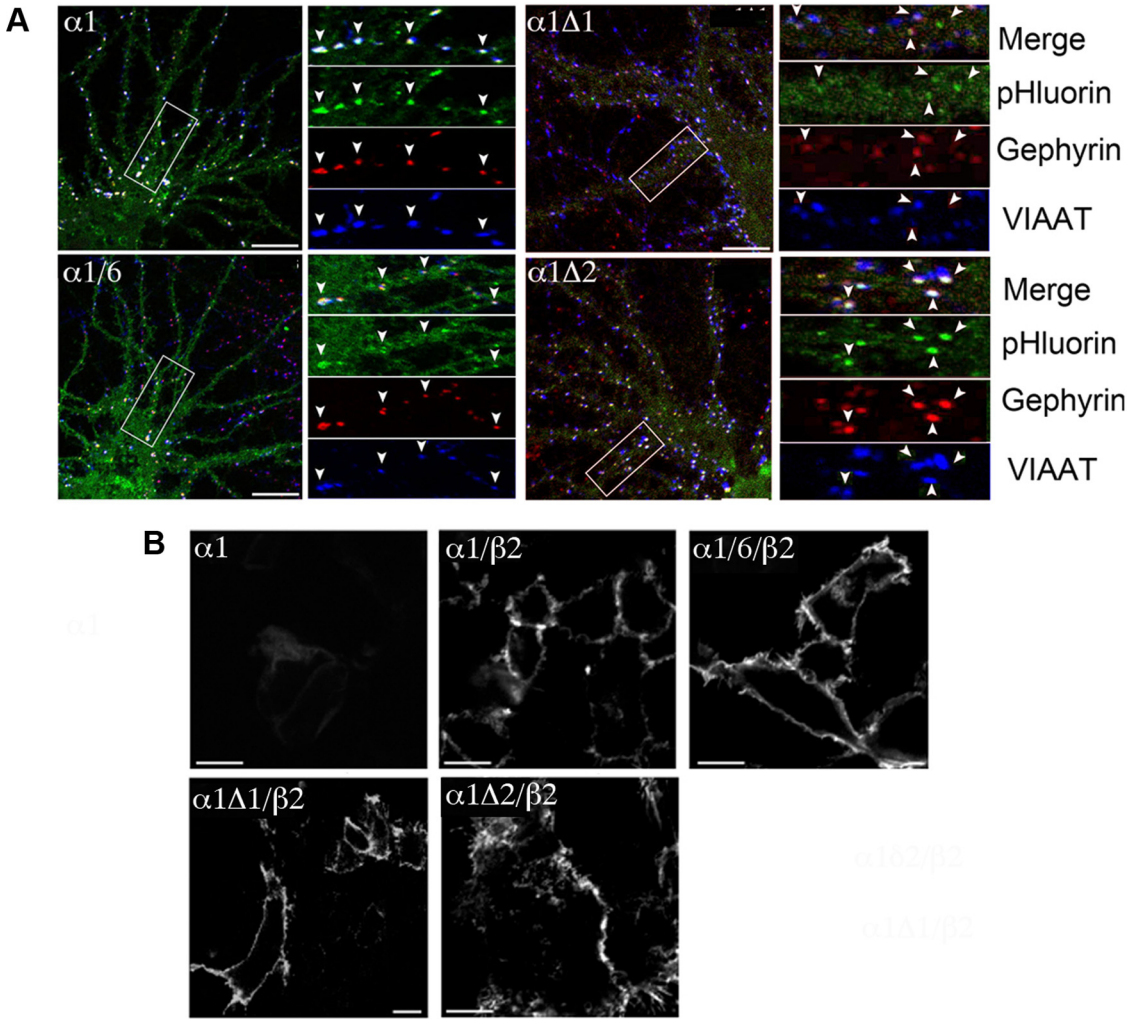

Figure 3. Preventing gephyrin binding to the α1 subunit disrupts GABA$_A$R synaptic clustering. ***A***, Nucleofected neurons (18–21 DIV) expressing GABA$_A$Rs incorporating $^{pH}\alpha$1 and $^{pH}\alpha$1/6 (left) or $^{pH}\alpha$1Δ1 and $^{pH}\alpha$1Δ2 subunits (right) were fixed, permeabilized, and stained with antibodies against gephyrin (red) and VIAAT (blue). Neurons were visualized via confocal microscopy, and the right panels represent enlargements of the boxed areas in the large panels. Arrowheads denote clusters. ***B***, HEK-293 cells expressing $^{pH}\alpha$1, $^{pH}\alpha$1/β2, $^{pH}\alpha$1/6/β2, $^{pH}\alpha$1Δ1/β2, or $^{pH}\alpha$1Δ2/β2 were fixed and stained with GFP antibodies without membrane permeabilization. Images were collected via confocal microscopy. Scale bars: 15 μm.

μm) was evident compared to those containing $^{pH}\alpha$1 subunits (2.9 ± 0.5 vs 9.4 ± 0.5; n = 40 and 38 neurons for $^{pH}\alpha$1 and $^{pH}\alpha$1/6, respectively; t test, $p \leq 0.001$). Significantly, there were no differences in the number of VIAAT-positive presynaptic terminals between neurons expressing α1 or α1/6 subunits. Moreover, we found that the ratio between gephyrin puncta and α1/6-subunit-containing clusters is at least 1.6 times (t test, $p \leq 0.014$) higher compare to α1-subunit-expressing neurons, suggesting no significant decrease in the number of inhibitory synapses. To confirm our experiments with $^{pH}\alpha$1/6 subunits, we examined the synaptic accumulation of GABA$_A$Rs incorporating $^{pH}\alpha$1Δ1 and $^{pH}\alpha$1Δ2 subunits (Fig. 3*A*, right). A significant decrease in the number of $^{pH}\alpha$1Δ1 synaptic clusters was seen compared to $^{pH}\alpha$1Δ2, (100 ± 3% vs 39.3 ± 3.2%; n = 15 and 14 neurons for $^{pH}\alpha$1Δ2 and $^{pH}\alpha$1Δ1, respectively; $p \leq 0.001$, t test). This result is consistent with our overlay assays which reveal that GST-Δ2 but not GST-Δ1 is capable of binding to gephyrin (Fig. 2).

To control for possible deleterious effects on receptor assembly, we examined the ability of the $^{pH}\alpha$1/6 subunit to gain access to the plasma membrane on coexpression with the β2 subunit in HEK-293 cells (Connolly et al., 1996). Transfected cells were stained with GFP antibodies without membrane permeabilization. Consistent with published data, access of the $^{pH}\alpha$1 subunit to the plasma membrane was dependent upon expression with β2 as measured by immunofluorescence. This experiment revealed that $^{pH}\alpha$1, $^{pH}\alpha$1/6, $^{pH}\alpha$1Δ1, and ^{pH} α1Δ2 subunits were incorporated into the plasma membrane at similar levels when expressed with β2. Collectively these studies suggest that residues 360–375 of the α1 subunit, which mediate direct binding to gephyrin, play a critical role in regulating the accumulation of GABA$_A$Rs at gephyrin-positive inhibitory postsynaptic specializations.

Mutating the gephyrin binding site in the α1 subunit modifies the properties of mIPSCs

To examine the effects of blocking gephyrin binding on the strength of synaptic inhibition, we compared the properties of mIPSCs in neurons expressing α1 subunit variants in which amino acids 360–375 had been either replaced or deleted. Nucleofected neurons that were identified via their endogenous green fluorescence were then subjected to patch-clamp recordings, and mIPSCs were isolated in the presence of TTX and glutamate receptor antagonists. Initially, we compared the properties of mIPSCs in neurons expressing $^{pH}\alpha$1Δ1 and

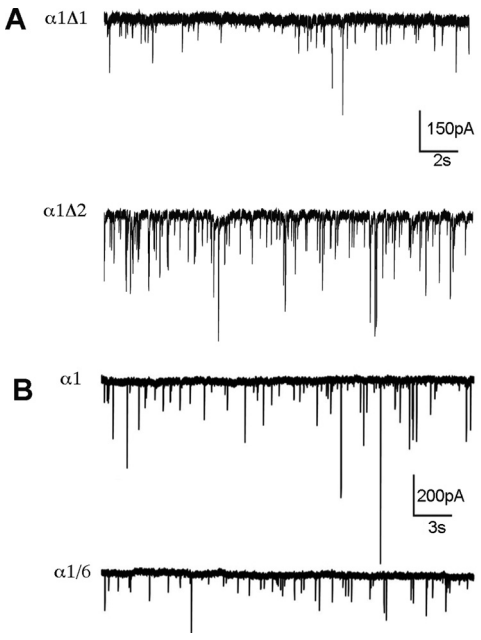

Figure 4. Preventing gephyrin binding to the α1 subunit decreases mIPSC amplitude. ***A***, ***B***, Sample traces are shown of mIPSCs recorded from 12 DIV neurons expressing either $^{pH}\alpha1\Delta1$ or $^{pH}\alpha1\Delta2$ subunits (***A***) or those expressing $^{pH}\alpha1$ or $^{pH}\alpha1/6$ subunits (***B***). These data were used to calculate mIPSC amplitude, frequency, rise, and decay times as detailed in the text.

$^{pH}\alpha1\Delta2$ constructs, because our biochemical and cell biological studies have shown that they differ in their ability to accumulate at inhibitory synapses. As neurons expressing $^{pH}\alpha1\Delta2$ do not exhibit a difference in clustering, mIPSC values from these cells were used as controls. Compared to neurons expressing $^{pH}\alpha1\Delta2$, the amplitude of mIPSCs was significantly reduced for those expressing $^{pH}\alpha1\Delta1$ ($p < 0.01$, *t* test; 122.5 ± 11. 3 pA for $^{pH}\alpha1\Delta2$, $n = 13$ vs 79.4 ± 7.0 pA for $^{pH}\alpha1\Delta1$, $n = 14$ neurons), whereas their frequency ($p = 0.8$, *t* test; 4.5 ± 1.2 vs 4.8 ± 0.9 Hz) and decay ($p = 0.5$, *t* test; 12.6 ± 0.7 vs 13.2 ± 0.6 ms) and rise ($p = 0.2$, *t* test; 0.44 ± 0.03 vs 0.51 ± 0.04 ms) times remained similar (Fig. 4*A*).

In a separate series of experiments, we also compared mIPSC properties in neurons expressing $^{pH}\alpha1/6$ and $^{pH}\alpha1$. Compared to neurons expressing $^{pH}\alpha1$, there was a significant decrease in the mean mIPSC amplitude in neurons expressing $^{pH}\alpha1/6$ ($p < 0.01$, *t* test; 139.7 ± 10.3 pA, $n = 25$ vs 102.9 ± 6.9 pA, $n = 23$ neurons). However, their frequency ($p = 0.09$, *t* test; 2.7 ± 0.6 vs 1.9 ± 0.6 Hz) and decay ($p = 0.7$, *t* test; 11.2 ± 0.6 vs 11.5 ± 0.5 ms) and rise ($p = 0.44$, *t* test; 0.54 ± 0.04 vs 0.59 ± 0.04 ms) times were similar (Fig. 4*B*).

Collectively, these results reveal that deleting or mutating residues 360–375 in the α1 subunit decreases mIPSC amplitude. This is consistent with our imaging studies that reveal a central role for these residues in regulating the stabilization of α1-subunit-containing $GABA_A$Rs at inhibitory synapses.

The binding of gephyrin to the α1 subunit is negatively regulated via threonine 375

Previous studies in yeast (Saiepour et al., 2010) have revealed that, in contrast to our findings presented here, the intracellular loops between TM helices 3 and 4 of the α2 and α3 subunits are capable of binding to the E-domain of gephyrin but not to the corresponding domain of the α1 subunit. A comparison of residues 360–375 within the α1 and α2 subunits reveals the presence of a nonconserved threonine residue (Thr375) followed by a proline residue within the α1 subunit. This fits the consensus sequence for phosphorylation by proline-directed kinases such as mitogen-activated and cyclin-dependent protein kinases (Fig. 5*A*) (Dhariwala and Rajadhyaksha, 2008) (probability in excess of 20%; http://www.cbs.dtu.dk/services/NetPhos/). To examine the role that Thr375 may play in regulating the binding of the α1 subunit to gephyrin, we initially used expression assays in yeast. Consistent with published studies, an interaction of a bait encoding the intracellular domains of the β subunit of GlyRs with gephyrin was evident as measured by β-galactosidase activity, while under the same conditions a bait encoding the intracellular domain of the α1 subunit was negative (Fig. 5*A*).

Mutation of Thr375 to alanine resulted in binding of the α1 subunit bait to gephyrin; however, mutations to either aspartate or glutamate, negatively charged residues that are often used to mimic the electrostatic effects of phosphorylation, were not able to interact with gephyrin (Fig. 5*A*,*B*). The mutation of Thr375 was specific because conversion of Ser373 or other residues surrounding Thr375 in the α1 subunit to their counterparts in the α2 subunit did not alter gephyrin binding. To support our findings in yeast, we created GST-fusion proteins in which Thr375 was mutated to aspartate or glutamate (GST-$\alpha1^{(T375D)}$ and GST-$\alpha1^{(T375E)}$, respectively) and to alanine. These fusion proteins were then tested for their ability to bind to gephyrin using an overlay assay. Mutation of Thr375 to aspartate or glutamate significantly reduced gephyrin binding (Fig. 5*B*) (68.9 ± 1.0%, $p \leq 0.001$ and 62.5 ± 6.1%, $p \leq 0.03$, respectively; *t* test; $n = 3$). In contrast, mutation to alanine did not appear to reduce the interaction with gephyrin (108.7 ± 5% of control; $p = 0.2$, *t* test; $n = 3$) (Fig. 5*B*).

In addition to the yeast two-hybrid data and *in vitro* binding assays, we performed ITC experiments to compare the relative affinities of α1, $\alpha1^{(T375A)}$, and $\alpha1^{(T375E)}$ for gephyrin. This revealed that the affinity of gephyrin for $\alpha1^{(T375E)}$ was reduced by ~10-fold compared to that for α1 (Fig. 5*C*) ($K_D = 183 \pm 33$ μM, $n = 2$ vs $K_D = 17 \pm 11$ μM, $n = 11$, respectively) (Table 1). In contrast, the affinity for $\alpha1^{(T375A)}$ was similar to that for α1 (Fig. 5*C*) ($K_D = 17 \pm 11$, $n = 11$ and $K_D = 36 \pm 11$ μM, $n = 2$, respectively) (Table 1). These results suggest a critical role of Thr375 in regulating the binding of the α1 subunit to gephyrin and further confirm the roles of residues 360–375 in mediating this interaction.

Thr375 regulates both the clustering of $GABA_A$Rs at synaptic sites and the properties of mIPSCs

Because our biochemical studies suggest that Thr375 plays an important role in determining the affinity of the α1 subunit for gephyrin, we compared the synaptic accumulation of $^{pH}\alpha1$ constructs in which this residue was mutated to aspartate residue ($^{pH}\alpha1^{(T375D)}$). Compared to $^{pH}\alpha1$, the number of clusters per 30 μm for $^{pH}\alpha1^{(T375D)}$ subunits was significantly reduced (Fig. 6*A*) (10.1 ± 0.7 and 3.0 ± 0.4; $p \leq 0.001$, *t* test; $n = 37$ and 43 neurons for $^{pH}\alpha1$ and $^{pH}\alpha1^{(T375D)}$, respectively). Consistent with our experiment with chimeric α1, we did not observe any significant change in the number of VIAAT-positive punctae between neurons expressing either α1 or $^{pH}\alpha1^{(T375D)}$ subunits. We have found that the ratio between gephyrin punctae and $^{pH}\alpha1^{(T375D)}$ subunit is at least 2.5 times (*t* test, $p < 0.001$) higher compared to α1-subunit-expressing neurons, suggesting that there is no significant change in the total number of inhibitory synapses.

We went on to analyze whether mimicking the phosphorylation of Thr375 had any effect on mIPSCs. Compared to wild-type

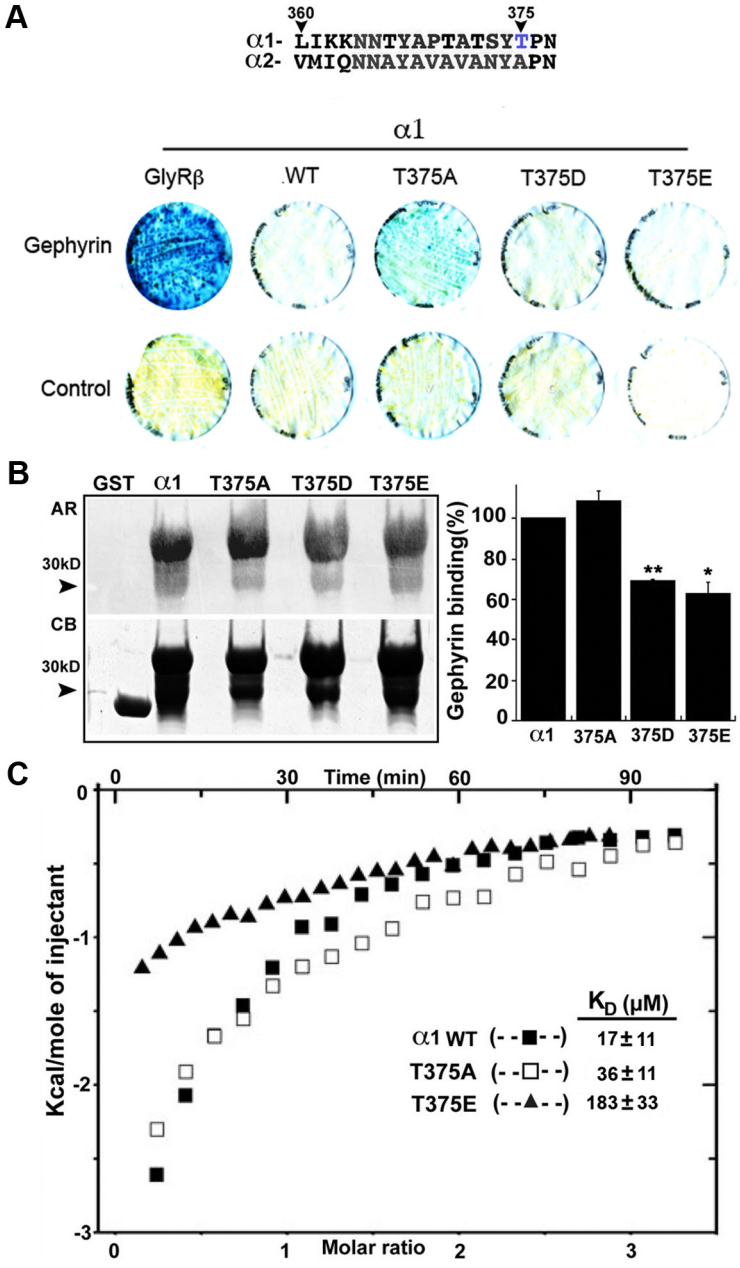

Figure 5. Thr375 regulates the affinity of the α1 subunit for gephyrin. ***A***, Alignment of residues 360–377 of the α1 and α2 subunits. Thr375 is highlighted in blue. Yeast transformants expressing gephyrin or control vector together with the intracellular domains of GlyR β or variants of α1 were assayed for β-gal activity. ***B***, GST-α1, α1T375A, α1T375D, and α1T375E were subjected to SDS-PAGE and overlaid with ^{35}S-gephyrin. Binding was visualized via autoradiography (left, top) and Coomassie staining (left, bottom). The level of gephyrin binding was then normalized to that seen for GST-α1 (100%; right). Data are presented as mean ± SEM. *$p < 0.05$; **$p < 0.01$ (unpaired *t* test; $n = 3$). ***C***, Binding affinities of gephyrin for α1 (■), α1T375A (□), and α1T375E (▲) as determined by ITC and representative titration curves are shown together with the average K_D values and their SDs.

lating both the number of GABA$_A$Rs at inhibitory synaptic sites and the strength of inhibitory synaptic transmission by regulating gephyrin binding. In addition, they suggest that phosphorylation of this residue may act as a modulatory mechanism to control the number of GABA$_A$Rs at inhibitory synapses.

Single-particle tracking reveals that gephyrin acts to increase the trapping of GABA$_A$Rs at inhibitory synapses

To investigate the influence of gephyrin on α1 GABA$_A$R surface dynamics, we used SPT on transfected hippocampal neurons expressing ^{pH}α1 or ^{pH}α1/6 subunits together with RFP-gephyrin that were labeled with low concentrations of QDs coupled to anti-GFP antibodies, a condition that facilitates the tracking of individual molecules (Bannai et al., 2006, 2009). The motions of QDs were characterized in both mRFP-gephyrin-positive and mRFP-gephyrin-negative structures (Fig. 7*A1*,*A2*) (Hanus et al., 2006). Cumulative analysis revealed that receptors containing ^{pH}α1 subunits showed significantly lower rates of diffusion compared to ^{pH}α1/6 (number of QDs analyzed, ^{pH}α1, $n = 327$; ^{pH}α1/6, $n = 290$; $p < 0.05$, Kolmogorov–Smirnov test) (Fig. 7*B*). However, at extrasynaptic sites, their rates of diffusion were similar (^{pH}α1, $n = 1326$; ^{pH}α1/6, $n = 1442$) (Fig. 7*B*, inset, outside gephyrin clusters). The QD movements were further analyzed by comparing the MSDs as a function of time (Bannai et al., 2006). At synapses, both subunits displayed confined movements, but higher confinement was seen for α1 compared to α1/6-containing receptors (Fig. 7*C*). To control variability, we determined the mean surface area explored by QDs over 1 s intervals of time for each quartile of the distribution in Figure 7*B*. Whereas the confinements of rapidly moving receptors (third and fourth upper quartiles of diffusion coefficients) were similar for both subunits, differences were seen for slower movements (lower quartiles) (Fig. 7*D*). The values in Figure 7*D* were normalized within each quartile. The actual surface areas explored in 1 s were as follows: first quartile, 3×10^{-3} and 7.2×10^{-3} μm^2; second quartile, 16.5×10^{-3} and 27.2×10^{-3} μm^2; third quartile, 45.8×10^{-3} and 63.1×10^{-3} μm^2; fourth quartile, 121.1×10^{-3} and 139.7×10^{-3} μm^2 (for ^{pH}α1 and ^{pH}α1/6, respectively; number of QD per quartile, ^{pH}α1, $n = 82$; ^{pH} α1/6, $n = 73$; *t* test between ^{pH}α1 and ^{pH}α1/6; first–third quartiles, $p < 0.001$; fourth quartile, not significant). The effect that was most pronounced for the slowest receptors thus indicated that the interaction with gephyrin was likely to be stronger for receptors moving more slowly. Furthermore, α1-containing receptors exhibited slightly shorter dwell time (mean,

^{pH}α1, amplitudes of mIPSCs for neurons expressing ^{pH}α1$^{(T375D)}$ subunits were significantly reduced ($p < 0.01$, *t* test; 192.2 ± 19.3 pA, $n = 8$, vs 113.1 ± 12.2 pA, $n = 17$, respectively) (Fig. 6*B*). In contrast, mutation of Thr375 had no significant effect on mIPSC frequency (*t* test, $p = 0.09$; 5.3 ± 1.8 vs 2.9 ± 0.4 Hz, respectively), and rise (*t* test, $p = 0.97$; 0.41 ± 0.03 vs 0.41 ± 0.04 ms, respectively) and decay (*t* test, $p = 0.73$; 7.8 ± 0.4 vs 8.1 ± 0.5 ms, respectively) times were also unaltered (Fig. 6*B*). These results thus suggest that mutating Thr375 to an aspartate residue modulates mIPSC properties primarily by a postsynaptic mechanism. Collectively, these results suggest that Thr375 plays a critical role in regu-

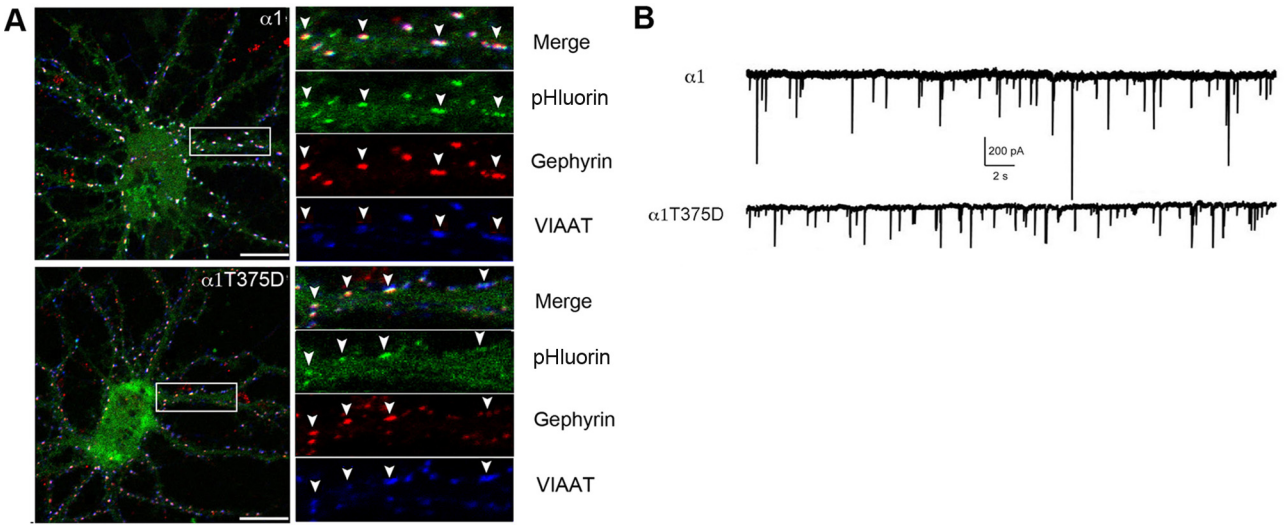

Figure 6. Thr375 regulates both the clustering of GABA$_A$Rs at inhibitory synapses and mIPSC amplitudes. ***A***, Nucleofected neurons (18–21 DIV) expressing GABA$_A$Rs incorporating $^{pH}\alpha1$ or $^{pH}\alpha1^{T375D}$ subunits were fixed, permeabilized, and stained with antibodies against gephyrin (red) and VIAAT (blue). Neurons were visualized via confocal microscopy and the right panels represent enlargements of the boxed areas at left with arrowheads pointing to clusters. Synaptic clustering of $^{pH}\alpha1^{T375D}$ was severely attenuated compared to $^{pH}\alpha1$-subunit-expressing neurons (for details, see text). ***B***, Typical traces of mIPSCs recorded from 12 DIV hippocampal neurons expressing $^{pH}\alpha1$ and $^{pH}\alpha1^{T375D}$ subunits. These data were then used to calculate mIPSC amplitude, frequency, rise, and decay times as detailed in the text.

$t = 7.4$ s) over gephyrin clusters compared to $\alpha1/6$-containing receptors (mean, $t = 8.9$ s) (Fig. 7*E*). The proportion of "stabilized" receptors remaining at synapses during the entire recording session (37.5 s) was also significantly higher ($p < 0.05$, two-tailed Fischer test) for $\alpha1$ subunits (11.8%) than for $\alpha1/6$ subunits (8%).

The theoretical dwell time of a molecule passing freely across a synapse with a stochastic motion was estimated to be about 5 s for a particle with a mean diffusion coefficient of 0.02 μm^2/s over an inhibitory synapse of ~0.1 μm^2 (with a measured diameter of ~300–400 nm; data not shown). In fact, the proportion of subunits dwelling >5 s at synapses (long dwell) was significantly higher ($p < 0.05$, one tailed Fischer test) for $\alpha1$ than for $\alpha1/6$ ($\alpha1$, 33.2% vs $\alpha1/6$, 28.2%). Analyses based on MSD and D parameters are limited by intrinsic averaging. To overcome this limitation and detect transient changes, we calculated the square steps (r^2) for 1 s time intervals along the trajectories. The distribution for QDs dwelling <5 s were unimodal (Fig. 7*E*, left inset). In contrast, the step distributions for long-dwelling QDs were bimodal, indicating that there were at least two modes of displacement within synapses (Fig. 7*E*, left inset). Compared to wild-type $\alpha1$, the step distributions for $\alpha1/6$ GABA$_A$Rs were shifted toward larger displacements. Thus, SPT reveals that the binding of the $\alpha1$ subunit to gephyrin is critical in mediating the transient stabilization of GABA$_A$Rs at synapses.

Discussion

Phasic inhibition in the brain is mediated largely via distinct subtypes of GABA$_A$Rs, the most abundant subtype of which contains $\alpha1$ subunits and accounts for in excess of 55% of benzodiazepine binding sites in the brain (McKernan and Whiting, 1996). However, our understanding of how neurons regulate their accumulation at inhibitory synapses remains rudimentary.

Gephyrin is a multifunctional protein and has been shown previously to regulate the synaptic clustering of GlyRs by mediating their binding to the cytoskeleton. Gephyrin also plays an essential role in synthesizing the molybdenum cofactor (Moco), an essential prosthetic group for a number of metabolic enzymes. Various additional binding partners of gephyrin have been identified, including components of the endocytic machinery and the exchange factor collybistin (Kirsch and Betz, 1995; Kins et al., 2000; Fuhrmann et al., 2002; Kneussel and Loebrich, 2007). Within the brain, gephyrin is highly enriched at inhibitory GABAergic synapses and colocalizes with receptor subtypes that contain $\alpha1$, $\alpha2$, or $\alpha3$ subunits (Sassoe-Pognetto and Fritschy, 2000; Alldred et al., 2005).

To directly address the role that gephyrin plays in the clustering of the most abundant benzodiazepine-sensitive GABA$_A$R subtypes in the brain, we used mature cultures of neurons that express high levels of both the receptor $\alpha1$ subunit and gephyrin. Using immunoprecipitation, we were able to establish that gephyrin is intimately associated with GABA$_A$Rs containing $\alpha1$ subunits and that this interaction is likely to occur at postsynaptic inhibitory specializations. To determine whether gephyrin is able to bind directly to the $\alpha1$ subunit, we used overlay assays, revealing that the intracellular domain of the $\alpha1$ and $\alpha2$ subunits but not the corresponding regions of the $\alpha5$ or $\alpha6$ subunits are able to bind directly to gephyrin. Given that the $\alpha1$ and $\alpha2$ subunits are synaptic, whereas the $\alpha5$ and $\alpha6$ subunits are largely extrasynaptic, these results suggest that direct binding of the $\alpha1$ and $\alpha2$ subunits to gephyrin mediates the synaptic clustering of the majority of GABA$_A$R subtypes.

Using ITC, we determined a K_D of ~20 μM for the binding of the $\alpha1$ subunit for gephyrin. While this affinity is significantly lower than that observed for the GlyR β subunit for gephyrin (Schrader et al., 2004), it is in line with the affinity of PDZ domains in scaffolds for their ligands, for example, the interaction between PDZ-containing proteins such as PSD-95 and their binding partners (Jemth and Gianni, 2007). The moderate affinity in the low micromolar range of GABA$_A$R $\alpha1$ subunits for gephyrin together with the detergent sensitivity of binding and possible modulation via phosphorylation are feasible explanations for why demonstrating the direct binding of these proteins in brain membranes has been problematic (Kittler et al., 2000, 2004).

By using deletion analysis and chimeras of the intracellular domain, we were able to establish that the binding of the $\alpha1$ subunit to the C-terminal E-domain of gephyrin is critically dependent on residues 360–375 of the $\alpha1$ subunit. These residues

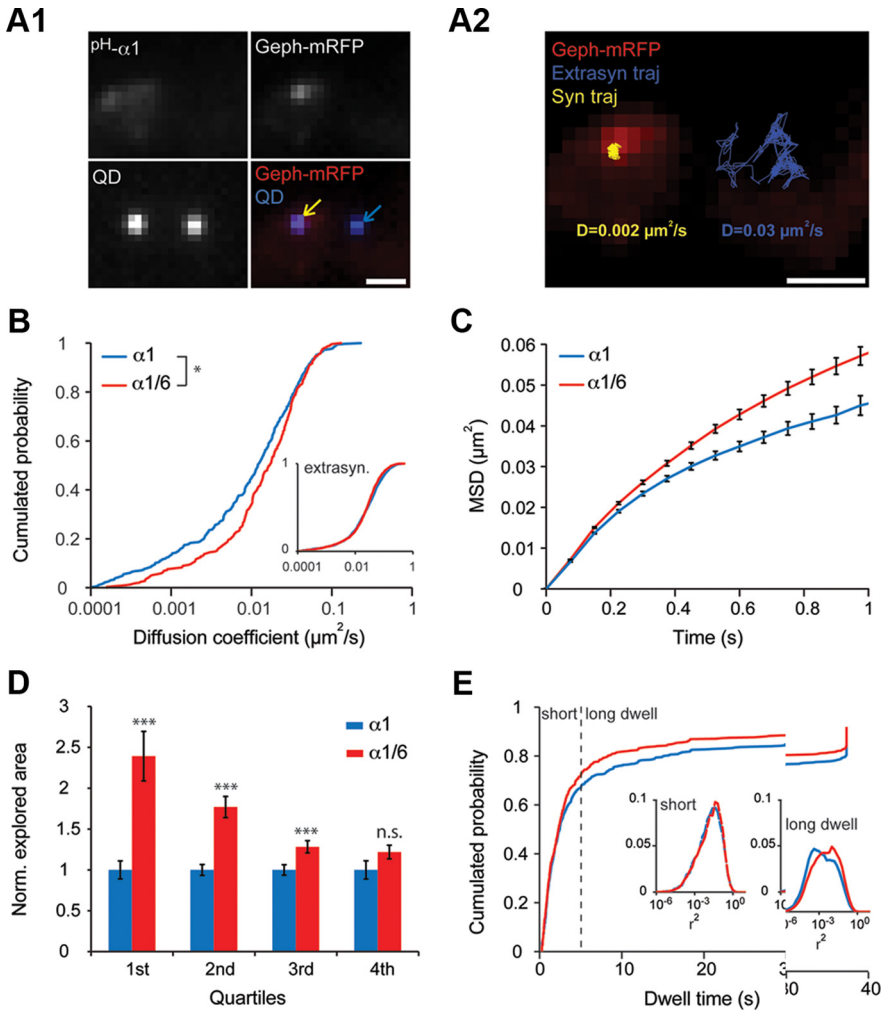

Figure 7. Analysis of the diffusion of α1 and α1/6 subunits using single-particle tracking. Hippocampal neurons were cotransfected with either $^{pH}\alpha$1 or $^{pH}\alpha$1/6 subunits and gephyrin-mRFP at 10 DIV. Subunits were tracked at 21 DIV with anti-GFP-coupled QDs. Inhibitory synapses were identified by the presence of cotransfected gephyrin-mRFP. ***A1***, ***A2***, Examples of trajectories of $^{pH}\alpha$1 subunits in living neurons. ***A1***, Codetection of $^{pH}\alpha$1 and gephyrin-mRFP. QD-coupled $^{pH}\alpha$1 subunits (blue dots) were visualized inside (yellow arrow) or outside (blue arrow) synapses (red). ***A2***, Individual trajectories reconstructed from QDs shown in ***A1***. Note that extrasynaptic subunits explored larger areas and moved faster (higher diffusion coefficients *D*) than synaptic ones. Scale bars: 1 μm. ***B***, The cumulative distribution of diffusion coefficients of the α1- and α1/6-subunit-containing GABA$_A$Rs showing the increased mobility of α1/6-type receptors at synapses. *$p < 0.05$ (Kolmogorov–Smirnov test). Inset, No difference could be seen outside synapses. ***C***, Average MSD of α1 and α1/6 GABA$_A$Rs at synapses. ***D***, Comparison of surface areas explored by α1- and α1/6-subunit-containing GABA$_A$Rs at synapses. QD trajectories were pooled according to their diffusion coefficients from the slowest (first) to the fastest (fourth) quartile. Note that the first and second lowest quartile groups exhibit a major increase for α1/6 compared to α1, and that this difference gradually decreases for faster subunits (first–third quartiles, ***$p < 0.001$; fourth quartile, not significant; *t* test). ***E***, Receptor dwell times at synapses. Note the longer dwell times for α1 than for α1/6 subunits. Insets, Distribution of square distances (steps) covered by QDs for 1 s time intervals along the trajectories. Distribution of steps for QDs dwelling for <5 s at synapses (left inset) or >5 s at synapses (right inset). Note the major shift toward greater displacements for long-dwelling α1/6 subunits.

are conserved in the α2 subunit, which is also capable of binding to gephyrin, but not in the intracellular domains of the α5 and α6 subunits. This structural conservation thus suggests a common mechanism for binding of GABA$_A$Rs to gephyrin. However, there appears to be little conservation between the amino acids that mediate the binding of the GlyR β subunit to gephyrin and those that mediate binding of the GABA$_A$R α1 subunit to this scaffold molecule. Higher-resolution structural studies are warranted to determine whether GABA$_A$Rs and GlyRs bind to the same domains in gephyrin.

To examine the functional significance of gephyrin binding, we used α1 expression constructs in which residues 360–375 were deleted or replaced with the corresponding region of the α6 subunit, which is unable to bind to gephyrin. This approach revealed that disrupting gephyrin binding to the α1 subunit severely reduced its ability to cluster at the postsynaptic sites. Consistent with this, the amplitude of the mIPSCs was reduced in neurons expressing α1/6 subunits compared to those expressing α1 subunits. Together, these results suggest a critical role for residues 360–375 of the α1 subunit in mediating the accumulation of α1 GABA$_A$Rs at the postsynaptic sites independent of somatic or dendritic compartments in cultured neurons. The corresponding region of the α2 subunit has also been shown to regulate clustering of the α2 GABA$_A$Rs at the postsynaptic sites including at the axon initial segment (AIS); however, it is likely that additional proteins (e.g., collybistin or neurofascin) are required along with gephyrin to selectively target GABA$_A$Rs at the AIS (Saiepour et al., 2010; Kriebel et al. 2011).

Recent studies in yeast have revealed that the intracellular loops of the α2 and α3 subunits are capable of binding to the E-domain of gephyrin but not to the corresponding region of the α1 subunit (Saiepour et al., 2010), in contrast to our findings, in which binding to the corresponding region of α1 was seen. To address this discrepancy, we used mutagenesis to convert nonconserved residues in the α1 subunit to their counterparts in α2. This revealed that mutation of Thr375, a predicted consensus site for phosphorylation by proline-directed kinases, was a key determinant in regulating the binding of the α1 subunit to gephyrin. Substitution with aspartate but not alanine reduced the affinity of gephyrin for the α1 subunit by ~10-fold as determined by ITC. Mutation to an aspartate also decreased the accumulation of the α1 subunit at inhibitory synapses together with the amplitude of mIPSCs. These results suggest that Thr375 plays a critical role in regulating binding to gephyrin and in controlling GABA$_A$R number at synaptic sites, further demonstrating the role of residues 360–375 in the α1 subunit for gephyrin binding. While it remains to be established that Thr375 is actually phosphorylated, these observations are suggestive of a role for phosphorylation in regulating gephyrin binding to the α1 subunit and thereby receptor accumulation at synapses. Intriguingly, the phosphorylation of Thr375 and its negative effects on gephyrin binding may provide an explanation for the inability of the intracellular domain of the α1 subunit to accumulate at inhibitory synapses when expressed in neurons compared to that of the α2 subunit (Tretter et al., 2008).

To provide mechanistic insights into how gephyrin regulates the synaptic accumulation of GABA$_A$Rs, we used SPT with QD-linked antibodies (Bannai et al., 2006). This approach in living neurons revealed that the interaction with gephyrin reduces the

diffusion and increases the confinement of the α1-subunit-containing $GABA_A$Rs only when located at gephyrin-positive inhibitory synapses. Consistent with this, the confinement of the α1 subunit at inhibitory synapses was also dependent on residues 360–375. To analyze the stability of $GABA_A$Rs, we compared the dwell times of α1 or α1/6 subunits. This revealed that, on average, the receptors incorporating α1 subunits exhibited slightly longer mean dwell times at inhibitory synapses compared to receptors containing α1/6 subunits. Furthermore, α1-containing receptors that spent longer times at synapses displayed smaller displacements than α1/6-containing receptors. These results suggest that receptors containing the α1 subunits interact with gephyrin, and that this binding is the result of a specific sequence.

Collectively our results suggest that the direct binding of gephyrin to the α1 subunit is a prerequisite for stabilizing $GABA_A$Rs at inhibitory synapses. Consistent with the results presented here, ablating gephyrin expression using RNA_i disrupts α1 subunit clustering in hippocampal neurons (Mukherjee and Moss, unpublished data). In contrast, the clustering of $GABA_A$Rs containing α1 subunits is not modified in cultured neurons from gephyrin knock-out mice (Levi et al., 2004). Significantly gephyrin knock-out mice die shortly after birth. Consistent with the multiple roles of gephyrin, reduced clustering of GlyRs and deficits in Moco biosynthesis are evident (Feng et al., 1998). Establishing a role for gephyrin in regulating $GABA_A$R clustering in these mice is a complex task given the likelihood of compensatory mechanisms. A possible explanation for the discrepancy between our studies, which clearly demonstrate that blocking binding to the α1 subunit inhibits synaptic accumulation, and the data from gephyrin knock-out mice is the recently identified protein muskelin (Heisler et al., 2011). Muskelin can bind to the α1 subunit and gephyrin and is important in regulating receptor trafficking. In the absence of gephyrin, muskelin may thus be able to stabilize α1 clusters on the neuronal membrane.

We have demonstrated that the synaptic accumulation of α1-subunit-containing $GABA_A$Rs, the principal mediators of phasic inhibition in the brain, is mediated via direct binding to gephyrin. This interaction depends on residues 360–375 of the α1 subunit that bind directly to the E-domain of gephyrin. This interaction limits $GABA_A$R diffusion at inhibitory synapses and thereby promotes receptor accumulation at these structures. Modulating this interaction via covalent modifications such as phosphorylation may be a potent mechanism to control the strength of fast GABAergic signaling.

References

Abramian AM, Comenencia-Ortiz E, Vithlani M, Tretter EV, Sieghart W, Davies PA, Moss SJ (2010) Protein kinase C phosphorylation regulates membrane insertion of GABA(A) receptor subtypes that mediate tonic inhibition. J Biol Chem 285:41795–41805.

Alldred MJ, Mulder-Rosi J, Lingenfelter SE, Chen G, Luscher B (2005) Distinct gamma2 subunit domains mediate clustering and synaptic function of postsynaptic GABAA receptors and gephyrin. J Neurosci 25:594–603.

Bannai H, Levi S, Schweizer C, Dahan M, Triller A (2006) Imaging the lateral diffusion of membrane molecules with quantum dots. Nat Protoc 1:2628–2634.

Bannai H, Levi S, Schweizer C, Inoue T, Launey T, Racine V, Sibarita JB, Mikoshiba K, Triller A (2009) Activity-dependent tuning of inhibitory neurotransmission based on GABAAR diffusion dynamics. Neuron 62:670–682.

Bedford FK, Kittler JT, Muller E, Thomas P, Uren JM, Merlo D, Wisden W, Triller A, Smart TG, Moss SJ (2001) GABA(A) receptor cell surface number and subunit stability are regulated by the ubiquitin-like protein Plic-1. Nat Neurosci 4:908–916.

Benke D, Fritschy JM, Trzeciak A, Bannwarth W, Mohler H (1994) Distribution, prevalence, and drug binding profile of gamma-aminobutyric acid type A receptor subtypes differing in the beta-subunit variant. J Biol Chem 269:27100–27107.

Bogdanov Y, Michels G, Armstrong-Gold C, Haydon PG, Lindstrom J, Pangalos M, Moss SJ (2006) Synaptic GABAA receptors are directly recruited from their extrasynaptic counterparts. EMBO J 25:4381–4389.

Brickley SG, Revilla V, Cull-Candy SG, Wisden W, Farrant M (2001) Adaptive regulation of neuronal excitability by a voltage-independent potassium conductance. Nature 409:88–92.

Brunig I, Scotti E, Sidler C, Fritschy JM (2002) Intact sorting, targeting and clustering of gamma-aminobutyric acid A receptor subtypes in hippocampal neurons *in vitro*. J Comp Neurol 443:43–55.

Connolly CN, Krishek BJ, McDonald BJ, Smart TG, Moss SJ (1996) Assembly and cell surface expression of heteromeric and homomeric gamma-aminobutyric acid type A receptors. J Biol Chem 271:89–96.

Connolly CN, Kittler JT, Thomas P, Uren JM, Brandon NJ, Smart TG, Moss SJ (1999) Cell surface stability of gamma-aminobutyric acid type A receptors. Dependence on protein kinase C activity and subunit composition. J Biol Chem 274:36565–36572.

Danglot L, Triller A, Bessis A (2003) Association of gephyrin with synaptic and extrasynaptic GABAA receptor varies during development in cultured hippocampal neurons. Mol Cell Neurosci 23:264–278.

Dhariwala FA, Rajadhyaksha MS (2008) An unusual member of the Cdk family: Cdk5. Cell Mol Neurobiol 28:351–369.

Essrich C, Lorez M, Benson JA, Fritschy JM, Luscher B (1998) Postsynaptic clustering of major GABAA receptor subtypes requires the gamma 2 subunit and gephyrin. Nat Neurosci 1:563–571.

Farrant M, Nusser Z (2005) Variations on an inhibitory theme: phasic and tonic activation of GABA(A) receptors. Nat Rev Neurosci 6:215–229.

Feng G, Tintrup H, Kirsch J, Nichol MC, Kuhse J, Betz H, Sanes JR (1998) Dual requirement for gephyrin in glycine receptor clustering and molybdoenzyme activity. Science 282:1321–1324.

Fischer F, Kneussel M, Tintrup H, Haverkamp S, Rauen T, Betz H, Wassle H (2000) Reduced synaptic clustering of GABA and glycine receptors in the retina of the gephyrin null mutant mouse. J Comp Neurol 427:634–648.

Fuhrmann JC, Kins S, Rostaing P, El Far O, Kirsch J, Sheng M, Triller A, Betz H, Kneussel M (2002) Gephyrin interacts with Dynein light chains 1 and 2, components of motor protein complexes. J Neurosci 22:5393–5402.

Glykys J, Mody I (2007) Activation of GABAA receptors: views from outside the synaptic cleft. Neuron 56:763–770.

Glykys J, Mann EO, Mody I (2008) Which GABA(A) receptor subunits are necessary for tonic inhibition in the hippocampus? J Neurosci 28:1421–1426.

Hanus C, Ehrensperger MV, Triller A (2006) Activity-dependent movements of postsynaptic scaffolds at inhibitory synapses. J Neurosci 26:4586–4595.

Harvey K, Duguid IC, Alldred MJ, Beatty SE, Ward H, Keep NH, Lingenfelter SE, Pearce BR, Lundgren J, Owen MJ, Smart TG, Luscher B, Rees MI, Harvey RJ (2004) The GDP-GTP exchange factor collybistin: an essential determinant of neuronal gephyrin clustering. J Neurosci 24:5816–5826.

Heisler FF, Loebrich S, Pechmann Y, Maier N, Zivkovic AR, Tokito M, Hausrat TJ, Schweizer M, Bahring R, Holzbaur EL, Schmitz D, Kneussel M (2011) Muskelin regulates actin filament- and microtubule-based GABA(A) receptor transport in neurons. Neuron 70:66–81.

Jacob TC, Bogdanov YD, Magnus C, Saliba RS, Kittler JT, Haydon PG, Moss SJ (2005) Gephyrin regulates the cell surface dynamics of synaptic GABAA receptors. J Neurosci 25:10469–10478.

Jacob TC, Moss SJ, Jurd R (2008) GABA(A) receptor trafficking and its role in the dynamic modulation of neuronal inhibition. Nat Rev Neurosci 9:331–343.

Jemth P, Gianni S (2007) PDZ domains: folding and binding. Biochemistry 46:8701–8708.

Kim EY, Schrader N, Smolinsky B, Bedet C, Vannier C, Schwarz G, Schindelin H (2006) Deciphering the structural framework of glycine receptor anchoring by gephyrin. EMBO J 25:1385–1395.

Kins S, Betz H, Kirsch J (2000) Collybistin, a newly identified brain-specific GEF, induces submembrane clustering of gephyrin. Nat Neurosci 3:22–29.

Kirsch J, Betz H (1995) The postsynaptic localization of the glycine receptor-associated protein gephyrin is regulated by the cytoskeleton. J Neurosci 15:4148–4156.

Kittler JT, Delmas P, Jovanovic JN, Brown DA, Smart TG, Moss SJ (2000)

Constitutive endocytosis of GABAA receptors by an association with the adaptin AP2 complex modulates inhibitory synaptic currents in hippocampal neurons. J Neurosci 20:7972–7977.

Kittler JT, Thomas P, Tretter V, Bogdanov YD, Haucke V, Smart TG, Moss SJ (2004) Huntingtin-associated protein 1 regulates inhibitory synaptic transmission by modulating gamma-aminobutyric acid type A receptor membrane trafficking. Proc Natl Acad Sci U S A 101:12736–12741.

Kneussel M, Betz H (2000) Clustering of inhibitory neurotransmitter receptors at developing postsynaptic sites: the membrane activation model. Trends Neurosci 23:429–435.

Kneussel M, Loebrich S (2007) Trafficking and synaptic anchoring of ionotropic inhibitory neurotransmitter receptors. Biol Cell 99:297–309.

Kneussel M, Brandstatter JH, Laube B, Stahl S, Muller U, Betz H (1999) Loss of postsynaptic GABA(A) receptor clustering in gephyrin-deficient mice. J Neurosci 19:9289–9297.

Kneussel M, Brandstatter JH, Gasnier B, Feng G, Sanes JR, Betz H (2001) Gephyrin-independent clustering of postsynaptic GABA(A) receptor subtypes. Mol Cell Neurosci 17:973–982.

Kriebel M, Metzger J, Trinks S, Chugh D, Harvey RJ, Harvey K, Volkmer H (2011) The cell adhesion molecule neurofascin stabilizes axo-axonic GABAergic terminals at the axon initial segment. J Biol Chem 286:24385–24395.

Levi S, Logan SM, Tovar KR, Craig AM (2004) Gephyrin is critical for glycine receptor clustering but not for the formation of functional GABAergic synapses in hippocampal neurons. J Neurosci 24:207–217.

Luscher B, Keller CA (2004) Regulation of GABAA receptor trafficking, channel activity, and functional plasticity of inhibitory synapses. Pharmacol Ther 102:195–221.

McKernan RM, Whiting PJ (1996) Which GABAA-receptor subtypes really occur in the brain? Trends Neurosci 19:139–143.

Pfeiffer F, Graham D, Betz H (1982) Purification by affinity chromatography of the glycine receptor of rat spinal cord. J Biol Chem 257:9389–9393.

Renner M, Choquet D, Triller A (2009) Control of the postsynaptic membrane viscosity. J Neurosci 29:2926–2937.

Rudolph U, Mohler H (2006) GABA-based therapeutic approaches: GABAA receptor subtype functions. Curr Opin Pharmacol 6:18–23.

Saiepour L, Fuchs C, Patrizi A, Sassoe-Pognetto M, Harvey RJ, Harvey K (2010) Complex role of collybistin and gephyrin in GABAA receptor clustering. J Biol Chem 285:29623–29631.

Sassoe-Pognetto M, Fritschy JM (2000) Mini-review: gephyrin, a major postsynaptic protein of GABAergic synapses. Eur J Neurosci 12:2205–2210.

Sassoe-Pognetto M, Kirsch J, Grunert U, Greferath U, Fritschy JM, Mohler H, Betz H, Wassle H (1995) Colocalization of gephyrin and GABAA-receptor subunits in the rat retina. J Comp Neurol 357:1–14.

Schrader N, Kim EY, Winking J, Paulukat J, Schindelin H, Schwarz G (2004) Biochemical characterization of the high affinity binding between the glycine receptor and gephyrin. J Biol Chem 279:18733–18741.

Sieghart W, Sperk G (2002) Subunit composition, distribution and function of GABA(A) receptor subtypes. Curr Top Med Chem 2:795–816.

Tretter V, Jacob TC, Mukherjee J, Fritschy JM, Pangalos MN, Moss SJ (2008) The clustering of GABA(A) receptor subtypes at inhibitory synapses is facilitated via the direct binding of receptor alpha 2 subunits to gephyrin. J Neurosci 28:1356–1365.

Triller A, Choquet D (2008) New concepts in synaptic biology derived from single-molecule imaging. Neuron 59:359–374.

Twelvetrees AE, Yuen EY, Arancibia-Carcamo IL, MacAskill AF, Rostaing P, Lumb MJ, Humbert S, Triller A, Saudou F, Yan Z, Kittler JT (2010) Delivery of GABAARs to synapses is mediated by HAP1-KIF5 and disrupted by mutant huntingtin. Neuron 65:53–65.

Yu W, Jiang M, Miralles CP, Li RW, Chen G, de Blas AL (2007) Gephyrin clustering is required for the stability of GABAergic synapses. Mol Cell Neurosci 36:484–500.